Uniform Silver Nanowires Synthesis by Reducing $AgNO_3$ with Ethylene Glycol in the Presence of Seeds and Poly(Vinyl Pyrrolidone)

Yugang Sun,[†] Yadong Yin,[‡] Brian T. Mayers,[†] Thurston Herricks,[‡] and Younan Xia*,[†]

Department of Chemistry and Department of Materials Science and Engineering, University of Washington, Seattle, Washington 98195

Received May 17, 2002. Revised Manuscript Received August 29, 2002

A solution-phase approach has been demonstrated for the large-scale synthesis of silver nanowires with diameters in the range of 30−40 nm, and lengths up to ∼50 μm. The first step of this process involved the formation of Pt (or Ag) nanoparticles by reducing $PtCl_2$ (or $AgNO_3$) with ethylene glycol (EG) heated to ∼160 °C. These Pt (or Ag) nanoparticles could serve as seeds for the heterogeneous nucleation and growth of silver (formed by reducing $AgNO_3$ with EG) because of their close match in crystal structure and lattice constants. In the presence of poly(vinyl pyrrolidone) (PVP), the growth of silver could be directed into a highly anisotropic mode to form uniform nanowires with aspect ratios as high as ∼1000. UV−visible spectroscopy, SEM, TEM, XRD, and electron diffraction were used to characterize these silver nanowires, indicating the formation of a highly pure phase, as well as a uniform diameter and bicrystalline structure. Both morphology and aspect ratios of these silver nanostructures could be varied from nanoparticles and nanorods to long nanowires by adjusting the reaction conditions, including the ratio of PVP to silver nitrate, reaction temperature, and seeding conditions. Measurements of the transport properties at room temperature indicated that these silver nanowires were electrically continuous with a conductivity (∼0.8×10^5 S/cm) approaching that of bulk silver.

Introduction

One-dimensional (1D) nanostructures (wires, rods, and tubes) are expected to play an important role in fabricating nanoscale devices. There are many applications where nanowires could be exploited to greatly enhance the functionality or performance of a material, including nanoelectronics, nanophotonics, formation of superstrong and tough composites, and fabrication of novel scanning probes.[1−3] As a result, the synthesis and characterization of nanowires have recently attracted attention from a broad range of researchers.[4] In particular, much effort has been devoted to the controlled synthesis of 1D nanostructures from metallic conductors because of their potential use as interconnects or active components in fabricating nanoscale devices.[5] Metallic nanowires may also provide a unique model system to experimentally probe physical phenomena such as quantized conductance and localization effects.[6]

Silver nanowires with well-defined dimensions represent a particular class of interesting nanostructures to synthesize and study because bulk silver exhibits the highest electrical and thermal conductivity among all metals. Silver is also an important material that has been used in a rich variety of commercial applications, and the performance of silver in these applications could be potentially enhanced by processing silver into 1D nanostructures (rather than as zero-dimensional (0D) nanoparticles) with controllable dimensions and aspect ratios. For example, the loading of silver in polymeric composites could be greatly reduced if nanoparticles were replaced by nanowires having higher aspect ratios.[7]

Although a number of approaches (such as those based on vapor−solid and vapor−liquid−solid processes) have been successfully developed for generating nanowires from semiconductors to dielectrics,[8−10] the most widely used method for generating metallic nanowires is still template-directed synthesis that involves either chemical or electrochemical depositions. A rich variety

[†] Department of Chemistry.
[‡] Department of Materials Science and Engineering.
* Corresponding author. E-mail: xia@chem.washington.edu.

(1) (a) Lieber, C. M. *Solid State Commun.* **1998**, *107*, 607. (b) Tans, S. J.; Devoret, M. H.; Dai, H.; Thess, A.; Smalley, R. E.; Geerligs, L. J.; Dekker, C. *Science* **1997**, *386*, 474. (c) Yang, P.; Lieber, C. M. *Science* **1996**, *273*, 1836. (d) Wong, S. S.; Joselevich, E.; Woolley, A. T.; Cheung, C.; Lieber, C. M. *Nature* **1998**, *394*, 52. (e) Dai, H.; Hafner, J. H.; Rinzler, A. G.; Colbert, D. T.; Smalley, R. E. *Nature* **1996**, *384*, 147.

(2) (a) Gudiksen, M. S.; Lauhon, L. J.; Wang, J.; Smith, D. C.; Lieber, C. M. *Nature* **2002**, *415*, 617. (b) Huang, Y.; Duan, X.; Cui, Y.; Lauhon, L. J.; Kim, K. H.; Lieber, C. M. *Science* **2001**, *294*, 1313. (c) Huang, Y.; Duan, X.; Wei, Q.; Lieber, C. M. *Science* **2001**, *291*, 630. (d) Duan, X.; Huang, Y.; Wang, J.; Lieber, C. M. *Nature* **2001**, *409*, 66.

(3) (a) Cui, Y.; Lieber, C. M. *Science* **2001**, *291*, 851. (b) Cui, Y.; Wei, Q.; Park, H. K.; Lieber, C. M. *Science* **2001**, *293*, 1289.

(4) See, for example, (a) Martin, C. R. *Science* **1994**, *266*, 1961. (b) Wu, C.-G.; Bein, T. *Science* **1994**, *266*, 1013. (c) Morales, A. M.; Lieber, C. M. *Science* **1998**, *279*, 208. (d) Hu, J.; Odom, T. W.; Lieber, C. M. *Acc. Chem. Res.* **1999**, *32*, 435.

(5) Prokes, S. M.; Wang, K. L. *MRS Bull.* **1999**, *24* (8), 13.

(6) (a) Zhang, Z.; Sun, X.; Dresselhaus, M. S.; Ying, J. Y. *Phys. Rev. B* **2000**, *61*, 4850. (b) Bockrath, M.; Liang, W.; Bozovic, D.; Hafner, J. H.; Lieber, C. M.; Tinkham, M.; Park, H. *Science* **2001**, *291*, 283.

(7) Carmona, F.; Barreau, F.; Delhaes, P.; Canet, R. *J. Phys. Lett.* **1980**, *41*, L-531.

10.1021/cm020587b CCC: $22.00
Published on Web 10/08/2002

of templates have already been demonstrated for use with such synthesis, including those made of both "hard" and "soft" materials. Typically, "hard" templates include channels contained in membrane of alumina[11] or track-etched polycarbonate;[12] pores within zeolite[13] or mesoporous silca;[14] carbon nanotubes;[15] and steps or edges supported on solid substrates.[16] Although these templates were effective in fabricating nanowires with uniform and controllable dimensions, many of them needed to be selectively dissolved under harsh conditions in order to harvest the nanowires. On the other hand, a range of "soft" templates have been demonstrated for use in the synthesis of metallic nanowires. Notable examples include polymer film of poly(vinyl alcohol) (PVA);[17] DNA chains;[18] mesostructures self-assembled from diblock copolymers;[19] rod-shaped micelles of cetyltrimethylammonium bromide (CTAB);[20] liquid crystalline phases of oleate[21] or sodium bis(2-ethylhexyl) sulfosuccinate (AOT)/*p*-xylene/water;[22] and arrays of calix[4]hydroquinone nanotubes.[23] The silver nanowires synthesized using these templates were often in the form of aggregated bundles, and the templates also needed to be removed in order to recover the individual nanowires. To avoid the step of template removal, several direct chemical and electrochemical approaches have been explored recently. For example, silver nanowires have been successfully synthesized by reducing $AgNO_3$ with a developer in the presence of AgBr nanocrystallites,[24] or by arc discharging between two silver electrodes immersed in an aqueous $NaNO_3$ solution.[25] Silver nanorods have been produced by irradiating an aqueous $AgNO_3$ solution with ultraviolet light in the presence of PVA,[26] or by electroreduction of $AgNO_3$ in aqueous solution with poly(ethylene glycol) (PEG).[27] The products of these templateless methods were, however, often characterized by problems such as relatively low yields, irregular morphologies, polycrystallinity, and low aspect ratios.

This article describes a soft (with temperatures <200 °C), solution-phase approach for the production of bicrystalline nanowires of silver with uniform diameters and in large quantities. The first step of this synthesis involved the formation of Pt (or Ag) seeds by reducing $PtCl_2$ (or $AgNO_3$) with ethylene glycol at ∼160 °C. Subsequently, solutions of $AgNO_3$ and poly(vinyl pyrrolidone) in ethylene glycol were added dropwise to this hot solution that contained metal seeds. Silver nanowires could nucleate and grow on these preformed seeds, with the number and length of these nanowires increasing over time. Like the so-called "polyol process", ethylene glycol served as both reducing agent and solvent in this synthesis.[28]

Experimental Section

Chemicals and Materials. Anhydrous ethylene glycol (EG, 99.8%), platinum chloride ($PtCl_2$, 99.99+%), silver nitrate ($AgNO_3$, 99+%), poly(vinyl pyrrolidone) (PVP, $M_W \approx 55\,000$), and acetone (HPLC grade) were purchased from Aldrich (Milwaukee, WI). All chemicals were used without further purification. Polished silicon (100) wafers (test grade, phosphorus-doped) were obtained from Silicon Sense (Nashua, NH). Pre-cleaned glass slides (micro slides 2947) were purchased from Corning Glass (Corning, NY). Either glass slides or silicon wafers covered with thermal oxide were employed as the substrates to fabricate gold electrodes for the conductivity test.

Preparation of Silver Nanowires. Silver nanowires were synthesized by reducing $AgNO_3$ with EG in the presence of Pt (or Ag) seeds and PVP. In a typical synthesis, 0.5 mL of $PtCl_2$ solution (1.5×10^{-4} M, in EG) was added to 5 mL of EG heated at ∼160 °C in a round-bottom flask (equipped with a condenser, thermocontroller, and magnetic stirring bar). After 4 min, 2.5 mL of $AgNO_3$ solution (0.12 M, in EG) and 5 mL of PVP solution (0.36 M, in EG) were added dropwise (simultaneously) to the hot solution over a period of 6 min. The reaction mixture was continued with heating at ∼160 °C until all $AgNO_3$ had been completely reduced. The growth of nanowires was monitored by sampling small portions of the reaction mixture at various reaction times, placing the samples on glass slides, and observing them under an optical microscope (in the dark-field mode). Vigorous stirring was maintained throughout the entire process. The product could be purified by centrifugation. In this case, the reaction mixture was diluted with acetone (5× by volume) and centrifuged at 2000 rpm for ∼20 min. The supernatant containing silver particles could be easily removed using a pipet. This centrifugation procedure could be repeated several times until the supernatant became colorless (silver nanoparticles had a yellow tint due to the surface plasmon resonance).

The simultaneous and dropwise addition of $AgNO_3$ and PVP solutions was critical to the formation of silver products with wire-like morphologies. Only the aforementioned procedure

(8) (a) Cui, Y.; Lauhon, L. J.; Gudiksen, M. S.; Wang, J.; Lieber, C. M. *Appl. Phys. Lett.* **2001**, *78*, 2214. (b) Gudiksen, M. S.; Lieber, C. M. *J. Am. Chem. Soc.* **2000**, *122*, 8801. (c) Duan, X.; Wang, J.; Lieber, C. M. *Appl. Phys. Lett.* **2000**, *76*, 1116.

(9) (a) Zheng, B.; Wu, Y.; Yang, P.; Liu, J. *Adv. Mater.* **2002**, *14*, 122. (b) Wu, Y.; Yang, P. *J. Am. Chem. Soc.* **2001**, *123*, 3165. (c) Huang, M.; Wu, Y.; Feick, H.; Tran, N.; Weber, E.; Yang, P. *Adv. Mater.* **2001**, *13*, 113.

(10) (a) Holmes, J. D.; Johnston, K. P.; Doty, R. C.; Korgel, B. A. *Science* **2000**, *287*, 1471. (b) Braun, E.; Eichen, Y.; Sivan, U.; Ben-Yoseph, G. *Nature* **1998**, *391*, 775.

(11) (a) Martin, B. R.; Dermody, D. J.; Reiss, B. D.; Fang, M.; Lyon, L. A.; Natan, M. J.; Mallouk, T. E. *Adv. Mater.* **1999**, *11*, 1021. (b) Zhang, Z.; Gekhtman, D.; Dresselhaus, M. S.; Ying, J. Y. *Chem. Mater.* **1999**, *11*, 1659.

(12) (a) Martin, C. R.; Mitchell, D. T. *Electroanal. Chem.* **1999**, *21*, 1. (b) Cepak, V. M.; Martin, C. R. *Chem. Mater.* **1999**, *11*, 1363.

(13) Edmondson, M. J.; Zhou, W.; Sieber, S. A.; Jones, I. P.; Gameson, I.; Anderson, P. A.; Edwards, P. P. *Adv. Mater.* **2001**, *13*, 1608.

(14) (a) Han, Y. J.; Kim, J. M.; Stucky, G. D. *Chem. Mater.* **2000**, *12*, 2068. (b) Huang, M. H.; Choudrey, A.; Yang, P. *Chem. Commun.* **2000**, 1063.

(15) (a) Ajayan, P. M.; Iijima, S. *Nature* **1993**, *361*, 333. (b) Ugarte, D.; Chatelain, A.; de Heer, W. A. *Science* **1996**, *274*, 1897.

(16) (a) Song, H. H.; Jones, K. M.; Baski, A. A. *J. Vac. Sci. Technol. A* **1999**, *17*, 1696. (b) Zach, M. P.; Ng, K. H.; Penner, R. M. *Science* **2000**, *290*, 2120.

(17) Bhattacharrya, S.; Saha, S. K.; Chakravorty, D. *Appl. Phys. Lett.* **2000**, *76*, 3896.

(18) (a) Braun, E.; Eichen, Y.; Sivan, U.; Ben-Yoseph, G. *Nature* **1998**, *391*, 775. (b) Eichen, Y.; Braun, E.; Sivan, U.; Ben-Yoseph, G. *Acta Polym.* **1998**, *49*, 663.

(19) (a) Zhang, D.; Qi, L.; Ma, J.; Cheng, H. *Chem. Mater.* **2001**, *13*, 2753. (b) Cornelissen, J. J. L. M.; van Heerbeek, R.; Kamer, P. C. J.; Reek, J. N. H.; Sommerdijk, N. A. J. M.; Nolte, R. J. M. *Adv. Mater.* **2002**, *14*, 489.

(20) (a) Jana, N. R.; Gearheart, L.; Murphy, C. J. *Chem. Commun.* **2001**, 617. (b) El-Sayed, M. A. *Acc. Chem. Res.* **2001**, *34*, 257. (c) Murphy, C. J.; Jana, N. R. *Adv. Mater.* **2002**, *14*, 80.

(21) Jiang, X.; Xie, Y.; Lu, J.; Zhu, L.; He, W.; Qian, Y. *J. Mater. Chem.* **2001**, *11*, 1775.

(22) Huang, L.; Wang, H.; Wang, Z.; Mitra, A.; Bozhilov, K. N.; Yan, Y. *Adv. Mater.* **2002**, *14*, 61.

(23) Hong, B. H.; Bae, S. C.; Lee, C.-W.; Jeong, S.; Kim, K. S. *Science* **2001**, *294*, 348.

(24) Liu, S.; Yue, J.; Gedanken, A. *Adv. Mater.* **2001**, *13*, 656.

(25) Zhou, Y.; Yu, S. H.; Cui, X. P.; Wang, C. Y.; Chen, Z. Y. *Chem. Mater.* **1999**, *11*, 545.

(26) Zhou, Y.; Yu, S. H.; Wang, C. Y.; Li, X. G.; Zhu, Y. R.; Chen, Z. Y. *Adv. Mater.* **1999**, *11*, 850.

(27) Zhu, J.-J.; Liao, X.-H.; Zhao, X.-N.; Chen, H.-Y. *Mater. Lett.* **2001**, *49*, 91.

(28) Fievet, F.; Lagier, J. P.; Figlarz, M. *MRS Bull.* **1989**, *December*, 29.

Table 1. Products Obtained When the Reactants Were Added Using Different Procedures[a]

sample no.	procedure	product
AG04	2.5 mL $AgNO_3$ and 5 mL PVP solutions were simultaneously injected using syringes within a period of ~6 min (the standard procedure as described in the *Experimental Section*)	a mixture of silver nanowires (~70%) and colloidal particles (~30%)
AG12	1 mL PVP solution was injected within 10 s before the addition of $AgNO_3$, and the $AgNO_3$ (2.5 mL) and PVP (4 mL) solutions were simultaneously injected in a period of 6 min	a mixture of silver nanorods (~10%) and particles (~90%)
AG35	5 mL PVP solution was injected within 10 s, and 2.5 mL $AgNO_3$ solution was then injected in a period of 10 s	silver nanoparticles only
AG36	5 mL PVP solution was injected within 10 s, and 2.5 mL $AgNO_3$ solution was then injected in a period of 6 min	silver nanoparticles only
AG38	2.5 mL $AgNO_3$ solution was injected in 10 s, and 5 mL PVP solution was then injected in a period of 6 min	a mixture of silver nanowires (~70%) and colloidal particles (~30%)

[a] Concentrations of $AgNO_3$ and PVP solutions were 0.12 and 0.36 M, respectively.

could lead to the formation of silver nanowires with relatively high aspect ratios and uniform diameters, and at relatively high yields. The major products obtained under different modes of solution addition are summarized in Table 1.

Instrumentation. The UV−visible extinction spectra were taken at room temperature on a Hewlett-Packard 8452 spectrometer (Palo Alto, CA) using a quartz cuvette with a 1-cm optical path. All the solutions had been diluted 30× with water before taking spectra. Optical images were captured using a Leica DMLM optical microscope equipped with a Polaroid digital camera (DMC-1, Boston, MA). The thermogravimetric analysis (TGA) was performed using a Shimazu TGA-50 thermobalance (Torrance, CA). The X-ray powder diffraction (XRD) patterns were recorded using a Philips PW1710 diffractometer with the Cu Kα radiation ($\lambda = 1.54056$ Å) at a scanning rate of 0.02 degrees per second in 2θ ranging from 30° to 80°. The samples for XRD were supported on glass substrates.

The scanning electron microscopic (SEM) measurements were carried out with a field emission microscope (FSEM, JEOL-6300F, Peabody, MA) at an acceleration voltage of 15 kV. In preparing the SEM samples, the reaction products were diluted by ~20× with water and then spotted on silicon substrates as small droplets. Copper grids coated with amorphous carbon film for transmission electron microscopic (TEM) studies were obtained from Ted Pella (Redding, CA). The TEM samples were prepared by placing small droplets of the diluted (by ~100× with water) reaction solutions on copper grids. All the TEM and SEM samples were allowed to dry at room temperature in a desiccator connected to vacuum pump. TEM images and electron diffraction patterns were taken using a JEOL-1200EX II microscope operated at 80 kV and a Philips EM-430 microscope operated at 200 kV. The diffraction patterns were recorded through selected-area electron diffraction on an individual nanowire (with a beam size of ~100 nm). High-resolution TEM (HRTEM) images were taken with a TOPCON 002B microscope operated at 160 kV.

Electrical Measurements. An interdigital array of gold electrodes (5-μm width and separated by 10 μm) was patterned on a SiO_2/Si wafer or glass slide using photolithography and selective wet etching. In a typical procedure, thin films of metals (300 nm of gold on the top of a 25-nm Ti/W adhesion layer) were deposited using an MRC 822 Sputtersphere (System Control Technology, Livermore, CA). Positive photoresist (AZ-1512, Clariant Corporation, Somerville, NJ) was then spin-coated on the gold surface, and patterned by exposure to UV light through an appropriate photomask. After developing in AZ-351 solution (Clariant, 1:4 dilution with water), the exposed regions of gold films were dissolved with aqua regia (HNO_3/HCl 1:3, in volume) and the unprotected underlayer of Ti/W was removed using an aqueous solution of hydrogen peroxide (30%). *Caution: these two wet etchants contain very strong oxidizing agents and should be handled with extreme care.* An individual silver nanowire was aligned onto the gold electrodes by applying the diluted (by ~100×) aqueous dispersion of these nanowires to one edge of a poly(dimethylsiloxane) (PDMS) stamp whose surface had been patterned with an array of channels. These channels were oriented parallel to the gold electrodes. By chance, a silver nanowire could be positioned against the edge of this stamp as the solvent drained through the channels. After the solvent had evaporated, the PDMS stamp was carefully peeled off from the gold electrodes, and the presence of silver nanowire could be confirmed using dark field optical microscopy. Silver epoxy (Chemtronics, Kennesaw, GA) was used to connect the gold pads with copper wires, which were subsequently connected (as shown later in Figure 10) to a Keithley 485 Auto Picoammeter (Keithkey Instruments, Clevland, OH) and a tunable DC power source (LL-9002-0V, Lamda Regulated Power Supply, Melville, NY). The electrical conductivity of this silver nanowire (at room temperature) could be calculated from the slope of its *I*-*V* curve.

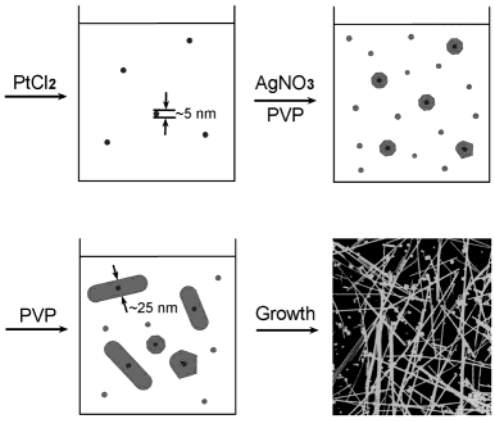

Figure 1. Schematic illustration of the experimental procedure that generates silver nanowires through a Pt-seeded polyol process.

Results and Discussion

Mechanism for the Formation of Silver Nanowires. The formation of anisotropic silver nanostructures involves at least two steps. Figure 1 shows a schematic diagram outlining the plausible mechanism. In the first step, Pt nanoparticles with diameters on the order of ~5 nm were formed by reducing $PtCl_2$ with ethylene glycol.

$$2HOCH_2{-}CH_2OH \rightarrow 2CH_3CHO + 2H_2O \quad (1)$$

$$2CH_3CHO + PtCl_2 \rightarrow CH_3CO{-}COCH_3 + Pt + 2HCl \quad (2)$$

In the second step, $AgNO_3$ and PVP were added dropwise to the reaction system, allowing the nucleation and growth of silver. Silver atoms (formed through the

reduction of $AgNO_3$ with EG) could nucleate through two different paths: heterogeneous and homogeneous nucleation. In the case of heterogeneous nucleation, the pre-synthesized Pt nanoparticles served as nuclei for the epitaxial growth of silver because their crystal structures and lattice parameters match closely. As a result of this nucleation process, silver nanoparticles with diameters of 20−30 nm were formed in the solution. At the same time, most silver atoms nucleated through the homogeneous nucleation process, yielding nanoparticles with diameters in the range of 1−5 nm. These silver nanoparticles were well-dispersed because of the presence of PVP, a polymeric surfactant that could chemically adsorb onto the surfaces of silver solid through O−Ag bonding.[29] It is well-known that the surface energies of large particles are lower than those of smaller ones. When this dispersion of bimodal silver nanoparticles was continuously heated at high temperatures, the small nanoparticles progressively disappeared to the benefit of larger ones via a process known as Ostwald ripening.[30] This ripening process for colloidal silver dispersions could take place with reasonable rates at a temperature as low as ∼85 °C.[31] The critical particle radius (below which a particle is not stable and should spontaneously dissolve) increased with temperature. As the reaction continued, the small silver particles were no longer stable in solution, and they started to dissolve and contribute to the growth of larger ones. With the assistance of PVP, some of the large nanoparticles were able to grow into rod-shaped structures with lateral dimensions in the range of 30−40 nm. The exact role of PVP in this process is not clear at the moment. One possible function for PVP is to kinetically control the growth rates of different crystalline faces by interacting with these faces through adsorption and desorption, which agrees with the "poisoning" mechanism. In this case, the "poison" adsorbed on some crystalline surfaces could significantly decrease their growth rates and lead to a highly anisotropic growth.[32] In principle, the growth process would continue until all the silver nanoparticles with diameters <5 nm were completely consumed, and only nanowires and the larger (more stable) nanoparticles survived.

A similar synthesis that involves $AgNO_3$ and PVP has also been extensively explored by Silvert et al., in which no Pt seeds was used.[31] In this case, silver nanoparticles having diameters <5 nm were formed through the homogeneous nucleation process; some large nanoparticles with diameters of ∼20 nm (∼5% of total population) were also formed at the early stage of this reaction. Even though the initial product was a mixture of silver nanoparticles similar to what we have observed in the early stage of our synthesis, no anisotropic structures were formed in their solution as the reactions proceeded. This difference could be attributed to the high molar ratios between the repeating unit of PVP and $AgNO_3$ (>10) that were used by these authors. As shown in their presented study, a heavy coverage of PVP on the surfaces of large silver nanoparticles might result in an isotropic growth for all different faces. In this regard, the concentration of PVP during the initial stage seems to play an important role in determining the morphologies of final products. Some evidence to support this argument can be derived from the results obtained when the reactants were added in different modes (Table 1). For example, dropwise addition of PVP to the reaction mixture was favorable for the formation of silver nanowires with high aspect ratios, whereas the morphology of the final products was not so sensitive to the addition rate of $AgNO_3$ (indicated by AG04 and AG38). If PVP was introduced to the reaction system before $AgNO_3$ was added and reduced, the products were predominated by nanoparticles (samples AG12, AG35, and AG36).

Microscopic Studies on the Formation of Silver Nanowires. The silver nanostructures at various stages of the growth process were characterized using both SEM and TEM. Figure 2 shows images of the samples that were taken from the reaction mixture after silver nitrate was added for 0, 10, 20, 40, 50, and 60 min. These images clearly show the evolution of silver nanostructures from 0D into 1D morphology over time at ∼160 °C, and correlate well with the mechanism sketched in Figure 1. Figure 2A gives a HRTEM image of some Pt nanoparticles that were spherical in shape with an average diameter of ∼5 nm. Their lattice fringes were spaced 0.23 nm apart, which is in good agreement with the *d* value for (111) planes of face-centered-cubic (fcc) platinum (0.226 nm). These platinum nanoparticles had a narrow distribution in size and could serve as seeds for the growth of fcc silver because of their close match in lattice constants. Once the solutions of $AgNO_3$ and PVP had been introduced to the reaction system, a bright yellow color immediately appeared, indicating the formation of silver nanoparticles or clusters through the reduction of $AgNO_3$ by EG. Figure 2B shows the initial product: a mixture of silver nanoparticles with two distinctive sizes. The majority of these nanoparticles had sizes <5 nm, and they were formed through homogeneous nucleation. Some larger nanoparticles (20−30 nm in diameter) were also present, which were formed through heterogeneous nucleation on the Pt seeds. When this colloidal dispersion was continued with heating at ∼160 °C, the small nanoparticles of silver spontaneously and slowly dissolved into the solution and recrystallized on the larger ones (Ostwald ripening[30]). After ∼20 min, the reaction mixture became opaque, and rodlike structures could be seen in the sample under an optical microscope (in the dark-field mode). As shown in Figure 2C, some of the large silver nanoparticles had, indeed, grown into rod-shaped anisotropic nanostructures with the assistance of PVP, while others kept growing into larger particles having a more isotropic morphology. In principle, this growth process should continue until all silver nanoparticles with diameters <5 nm had been completely consumed (Figure 2D, E, and F). Both the length and number of silver nanowires increased with the elongation of reaction (or growth) time. In a typical synthesis, nanowires obtained at 40 min were very short with lengths <3 μm (Figure 2D),

(29) Huang, H. H.; Ni, X. P.; Loy, G. L.; Chew, C. H.; Tan, K. L.; Loh, F. C.; Deng, J. F.; Xu, G. Q. *Langmuir* **1996**, *12*, 909.

(30) (a) Roosen, A. R.; Carter, W. C. *Physica A (Amsterdam)* **1998**, *261*, 232. (b) Matijevic, E. *Chem. Mater.* **1993**, *5*, 412.

(31) (a) Silvert, P.-Y.; Herrera-Urbina, R.; Duvauchelle, N.; Vijayakrishnan, V.; Elhsissen, K. T. *J. Mater. Chem.* **1996**, *6*, 573. (b) Silvert, P.-Y.; Herrera-Urbina, R.; Tekaia-Elhsissen, K. *J. Mater. Chem.* **1997**, *7*, 293.

(32) (a) Almeida, M.; Alcacer, L. *J. Crystal Growth* **1983**, *62*, 183. (b) Iguchi, M.; Murase, I. *J. Cryst. Growth* **1974**, *24/25*, 596.

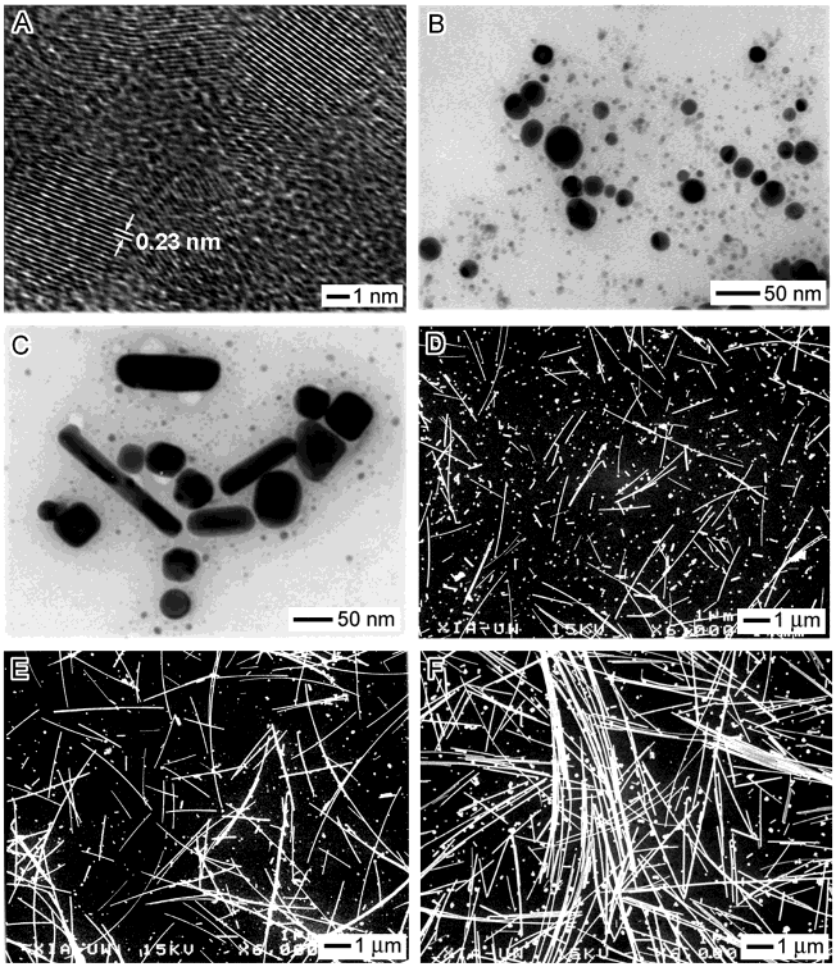

Figure 2. (A) HRTEM image of platinum seeds with sizes of ~5 nm. The lattice fringes are spaced 0.23 nm apart, which is in agreement with the *d* value of the (111) planes of fcc platinum. (B, C) TEM and (D−F) SEM images of five samples, showing different stages of growth for silver nanowires. These samples were prepared by taking a small portion from the reaction mixture at (B) 10, (C) 20, (D) 40, (E) 50, and (F) 60 min. The concentrations of $AgNO_3$, PVP, and $PtCl_2$ were 0.12, 0.36, and 1.5×10^{-4} M, respectively. The reaction temperature was controlled at 160 °C.

and they could grow up to 20−50 μm in length after the reaction had proceeded for 60 min (Figure 2F).

Spectroscopic Monitoring of the Wire Growth Process. The UV−visible spectroscopic method can also be used to track the morphological evolution involved in the growth process because silver nanostructures having different shapes exhibit surface plasmon resonance (SPR) bands at different frequencies.[33] Figure 3 compares the UV−visible extinction spectra obtained from solutions sampled at different reaction times (after the addition of $AgNO_3$ and PVP). Figure 3A shows the variation of extinction spectra between silver nanorods with low aspect ratios and silver nanoparticles. The appearance of a weak plasmon peak at ~410 nm (curve *a*) indicated the formation of silver colloids with nanometer-sized dimensions. This peak exhibited a broad full-width at half-maximum (fwhm) of ~100 nm and the tailing effect, indicating the existence of a broad distribution in size and morphology for these silver nanoparticles.[34] As the reaction proceeded from 10 to 12 min, the intensity of this peak decreased slightly and a new peak at a longer wavelength (~530 nm) appeared. This red-shift in energy implies the formation of rodlike structures, whose longitudinal plasmon resonance could contribute to the appearance of a peak at wavelengths longer than 410 nm.[20a] When the reaction had proceeded for 20 min, more silver nitrate was reduced and the silver nanorods continued to grow in length. The longitudinal SPR mode for these nanorods was further red-shifted from 530 to 570 nm (curves *b*−*e*), whereas the peak around 410 nm was slightly blue-shifted from 413 to 404 nm. These results were consistent with theoretical predictions: as the aspect ratio increases, the longitudinal SPR band (λ_L) should be red-shifted significantly, whereas the transverse SPR (λ_T) band shifts only slightly to the blue side.[35]

Figure 3B shows the UV−visible spectra of solutions sampled from the reaction mixture with the growth times scattered around 30 min. (Note that different scales of extinction intensity were used in panels A, B, and C of Figure 3.) In the period from 20 to 28 min, the longitudinal SPR band of nanorods did not exceed 570 nm even though their growth continued to proceed. Between 28 and 29 min, this SPR peak was still positioned around 570 nm, although a significant in-

(33) (a) Kerker, M. *J. Colloid Interface Sci.* **1985**, *105*, 297. (b) Sarkar, D.; Halas, N. J. *Phys. Rev. E* **1997**, *56*, 1102.
(34) (a) Kreibig, U.; Genzel, L. *Surf. Sci.* **1985**, *156*, 678. (b) Granqvist, C. G.; Buhrman, R. A. *J. Appl. Phys.* **1976**, *47*, 2200.
(35) (a) Link, S.; Mohamed, M. B.; El-Sayed, M. A. *J. Phys. Chem. B* **1999**, *103*, 3073. (b) Ah, C. S.; Hong, S. D.; Jang, D.-J. *J. Phys. Chem. B* **2001**, *105*, 7871.

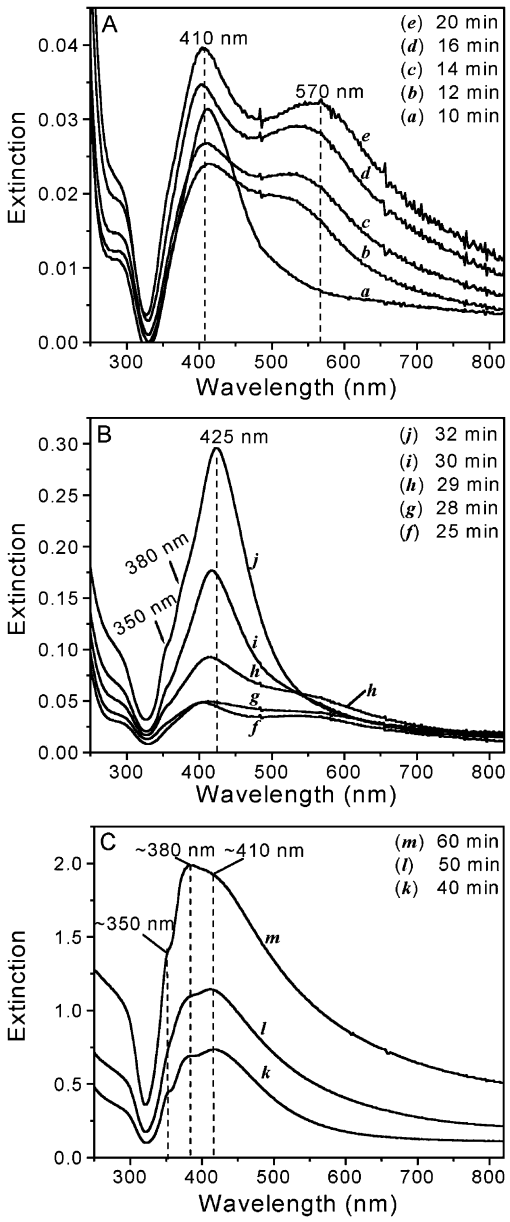

Figure 3. UV−visible extinction spectra of the reaction mixture at various reaction times: (*a*) 10, (*b*) 12, (*c*) 14, (*d*) 16, (*e*) 20, (*f*) 25, (*g*) 28, (*h*) 29, (*i*) 30, (*j*) 32, (*k*) 40, (*l*) 50, and (*m*) 60 min. All these solutions had been diluted by 30× with highly purified water before taking spectra. The extinction peaks at 350, 380, 410, and 570 nm could be attributed to the surface plasmon resonance of silver with different origins: the longitudinal mode of nanowires similar to that of bulk silver, the transverse mode of nanowires, nanoparticles, and the longitudinal mode of nanorods. Reaction conditions were the same as those indicated in Figure 2.

crease in intensity was observed. This result indicated that the silver nanorods increased in number without apparent growth in length. As the reaction proceeded from 29 to 30 min, the SPR peak at ∼570 nm decreased in intensity and eventually disappeared from the visible regime, indicating the formation of silver nanorods/nanowires with aspect ratios greater than 5.[35b] At the same time, the extinction intensity around 410 nm abruptly increased by approximately 2-fold. This large change in the optical spectra implied that the growth rate of silver nanorods could be greatly accelerated once a critical concentration of nanorods had been reached. Moreover, the peak positioned at ∼410 nm slightly shifted to the red, indicating an increase in size for both silver nanorods and nanoparticles.[36] The extinction peak for λ_T would blue-shift from ∼410 to ∼380 nm as the average length of the silver nanorods and nanowires was increased.[17,27] Therefore, the shoulder peak at ∼380 nm could be considered as the optical signature of relatively long silver nanowires, which started to appear in the reaction mixture after the reactants had been added for ∼32 min. At this point, optical signatures similar to those of bulk silver also began to appear, as indicated by the shoulder peak around 350 nm.

Figure 3C shows the change in extinction spectra at longer reaction times, characterized by the further elongation of silver nanorods. As the length of these nanorods increased with time, the two SPR peaks at 380 and 350 nm were further increased in intensity relative to the peak positioned at ∼410 nm. Nevertheless, the peak at ∼410 nm (this peak shifted to the red as the reaction proceeded) still existed even after the reaction solution had been heated for 60 min or longer (curve *m* in Figure 3C). This observation suggests that the final product of our synthesis should be a mixture of silver nanowires and colloidal particles, which is consistent with our electron microscopic studies shown in Figure 2F.

Structural Characterization of the Silver Nanowires. Although the final product of a typical synthesis contained both silver nanowires and nanoparticles, this mixture could be readily separated through centrifugation to obtain a pure sample of nanowires. Figure 4A shows the UV−visible extinction spectra before and after three cycles of centrifugation and separation of the product obtained at 60 min. In this case, the precipitate exhibited two SPR peaks (∼380 and ∼350 nm), and both of them belong to the optical signatures of silver nanowires. The supernatant, on the other hand, displayed a broad peak around 436 nm, which could be attributed to the SPR band of silver nanoparticles. Figure 4B shows the SEM image of silver nanowires after purification, clearly indicating the removal of silver nanoparticles from this sample. These nanowires had a mean diameter of ∼38 nm, with a standard deviation of ∼5 nm. The image also shows the straightness along the longitudinal axis, the level of perfection, and the copiousness in quantity that we could routinely achieve using this synthetic approach. Figure 4C shows the TEM image of several such nanowires, indicating the uniformity in diameter along each individual wire. The XRD pattern (Figure 4D) taken from a large quantity of sample suggested that silver nanowires synthesized using this solution-phase method existed purely in *fcc* phase. The lattice constant calculated from this XRD pattern was 4.092 Å, which is very close to the reported data (a = 4.0862 Å, JCPDS File 04-0783). It is worth noting that the ratio of intensity between (111) and (200) peaks exhibits a relatively high value of 3 (the theoretical ratio is 2.5), indicating the enrichment of {111} crystalline planes in the silver nanowires.

The crystal structure of these silver nanowires was further studied using TEM and electron diffraction. Previous studies have suggested a low threshold for

(36) Bohren, C. F.; Huffman, D. R. *Absorption and Scattering of Light by Small Particles;* Wiley: New York, 1983.

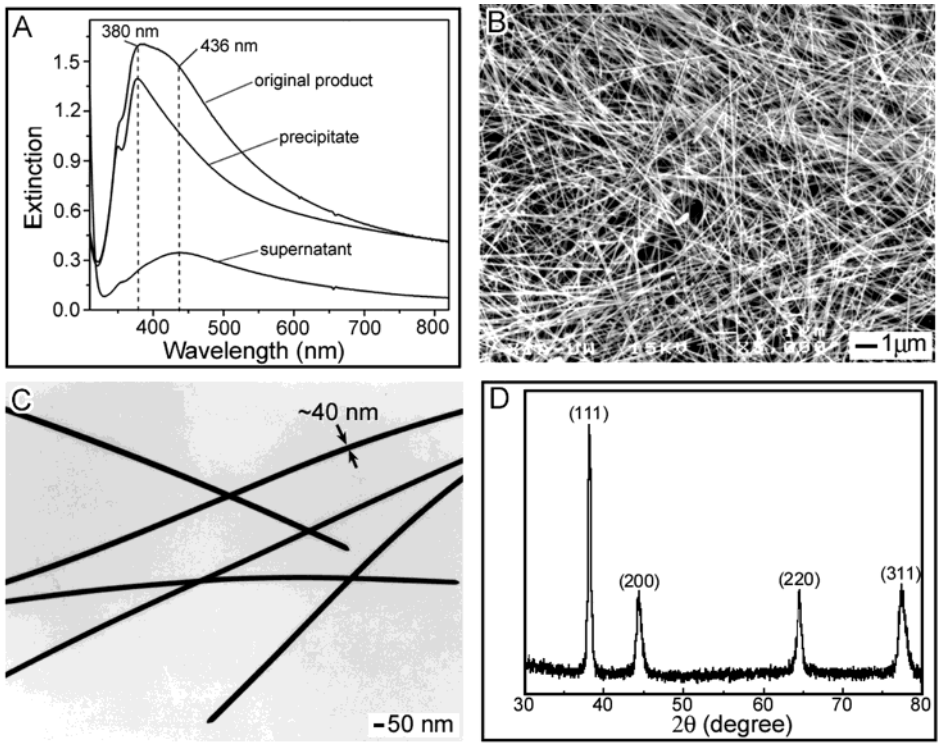

Figure 4. (A) UV−visible extinction spectra of the final product before and after three cycles of centrifugation and separation. (B) SEM and (C) TEM images of a purified sample of silver nanowires. (D) XRD pattern of as-synthesized silver nanowires (~40 nm diameter). All the peaks could be indexed to fcc silver. Reaction conditions were the same as those indicated in Figure 2.

twining along {111} planes for fcc metals such as silver and gold, especially when their 1D nanostructures have relatively high aspect ratios.[37] These nanostructures tend to grow as bicrystals twined along the {111} planes. Figure 5A shows a bright field TEM image of the end of an individual silver nanowire with its twin plane parallel to the longitudinal axis (as indicated by an arrow). Figures 5B and 5C are dark field TEM images illustrating the twin structure of this wire. The dark field image shown in Figure 5B is formed from a {111} diffracted beam showing one domain of the bicrystal. When the electron beam was tilted to form the image from {002t} spots, the dark field image shown in Figure 5C illustrates the adjacent domain of this bicrystal. It should be noted that in these images the nanowire was illuminated by a highly convergent beam which covered only the lower half of the wire. The contrast present in these images can be attributed to defect-induced strains. Thickness fringes are also visible toward the end of this wire. Figure 5D shows the corresponding selected-area diffraction pattern obtained with the beam parallel to [110] axis. This pattern is characteristic of reflection twins in an fcc metal. The pattern displays reflection symmetry about the {111}-type plane. The interpenetrating patterns correspond to the crystals on either side of the twin (as indexed).

Influence of the Ratio between PVP and $AgNO_3$. The morphology and aspect ratio of the silver nanowires strongly depended on the molar ratio between the repeat unit of PVP and $AgNO_3$. Figure 6A shows the TEM image of a sample that was synthesized using a procedure similar to the standard synthesis (shown in Figures 2−5), except that the molar ratio of PVP to $AgNO_3$ increased from 6 to 18. In this case, silver nanoparticles with an average size of ~20 nm were obtained as the major product. No nanorods or wires were formed even after the solution had been heated at 160 °C for 5 h. The relatively high molar ratio of PVP to $AgNO_3$ might cause high coverage of PVP on all faces of the seeds, leading to an isotropic growth mode. Figure 6B presents an SEM image of the product obtained using a PVP/$AgNO_3$ ratio of 1.5. The resultant nanowires had a thicker average diameter (~100 nm) than the samples shown in Figures 2−5, as well as relatively rougher surfaces. In this case, the low ratio of PVP to $AgNO_3$ caused a decrease in coverage not only for the fast-growing end faces, but also for the side surfaces of each nanowire. The incomplete coverage of PVP on side surfaces could not effectively passivate these faces, and the nanowires became thicker (due to lateral growth) while they grew longer.

Influence of Reaction Temperature. Temperature was also found to play an important role in the formation of silver nanowires. Figure 7 shows the SEM images of silver products synthesized at different reaction temperatures. When the reaction mixture was heated at 100 °C for more than 20 h (Figure 7A), no nanowires were formed. The reduced silver formed nanoparticles with polydispersed sizes and shapes. It seemed that the relatively low reaction temperature could not provide enough energy required for the activation of specific faces for the anisotropic growth of nanowires. Both the dissolution of small silver nanoparticles and the diffusion of silver atoms on the surface of silver nanorods or nanowires should require a relatively high temperature. Conversely, over-high temperatures seemed to favor the

(37) (a) Wang, Z. L.; Mohamed, M. B.; Link, S.; El-Sayed, M. A. *Surf. Sci.* **1999**, *440*, L809. (b) Bögels, G.; Meekes, H.; Bennema, P.; Bollen, D. *J. Phys. Chem. B* **1999**, *103*, 7577. (c) Link, S.; Wang, Z. L.; El-Sayed, M. A. *J. Phys. Chem. B* **2000**, *104*, 7867.

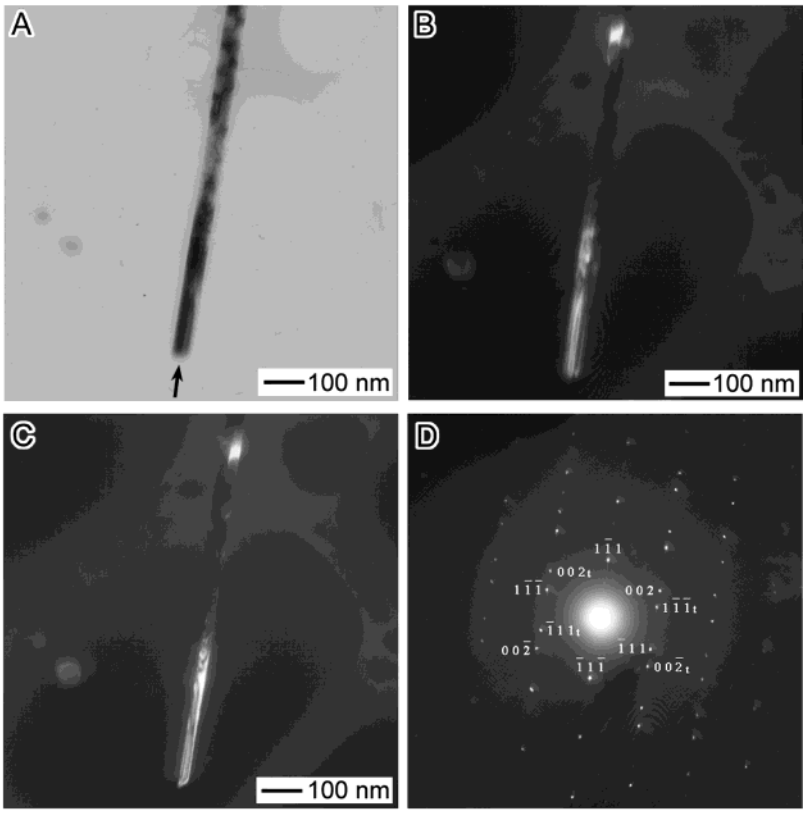

Figure 5. (A) Bright field TEM image of the end of an individual silver nanowire, showing the bicrystallinity that is characteristic of nanowires synthesized using the present method. The (111) twin plane in the middle of this nanowire is indicated by an arrow. (B, C) Dark field TEM images of the same nanowire imaged by tilting the electron beam parallel to the [110] axis. (D) The corresponding convergent beam electron diffraction pattern. Indices without subscript refer to the left side of the nanowire shown in (B), and indices with the subscript "t" refer to the right side. These two patterns have the reflection symmetry about the {111}-type planes.

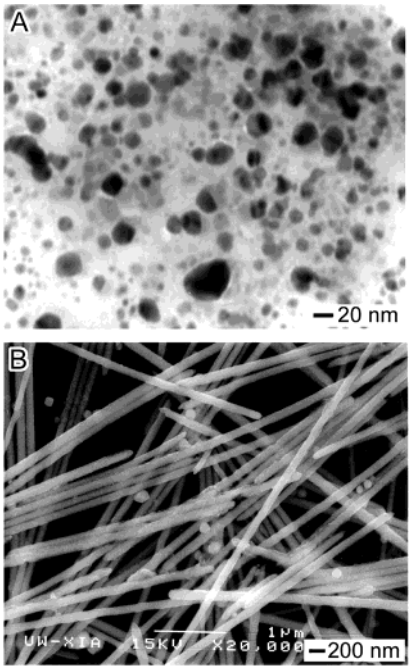

Figure 6. SEM images of two as-synthesized products, showing the variation of morphology when the molar ratio between PVP and $AgNO_3$ was changed. (A) $n_{PVP}/n_{AgNO3} = 18$; (B) $n_{PVP}/n_{AgNO3} = 1.5$. Other conditions were the same as those indicated in Figure 2.

formation of silver nanowires with low aspect ratios. Figure 7B shows the SEM image of silver nanorods that were grown around 185 °C. These nanorods had a mean diameter of 39 ± 3 nm, and an average length of 1.9 ± 0.4 μm. The length of these nanorods had dramatically decreased (by ~90%) in comparison with the nanowires synthesized at 160 °C. Electron diffraction patterns obtained from these silver nanorods indicated that they were also bicrystalline in structure.

Influence of Seeding Conditions. Because our synthesis involves a heterogeneous nucleation process, the seeding conditions are expected to influence the dimensions of silver nanowires. Concentration, size distribution, and crystalline structure of the platinum seeds were all found to play certain roles. Figure 8A shows a TEM image of the sample that was synthesized using a procedure similar to that used in the standard synthesis (Figures 2−5). In this case, however, the initial concentration of $PtCl_2$ was increased by ~10 times. As a result, the diameter of silver nanowires was reduced from ~40 to ~30 nm due to an increase in the number of Pt seeds. The main reason was that the source of small silver nanoparticles (with diameter <5 nm) was kept constant, leading to a decrease in the average amount of material available for nanowire growth. Electron diffraction patterns taken from individual nanowires indicated that these thin nanowires were also bicrystalline. The independence of crystalline structure of silver nanowires regardless of their dimensions implied that the bicrystalline structure was probably the most stable form for 1D nanostructures of metals with *fcc* structure.

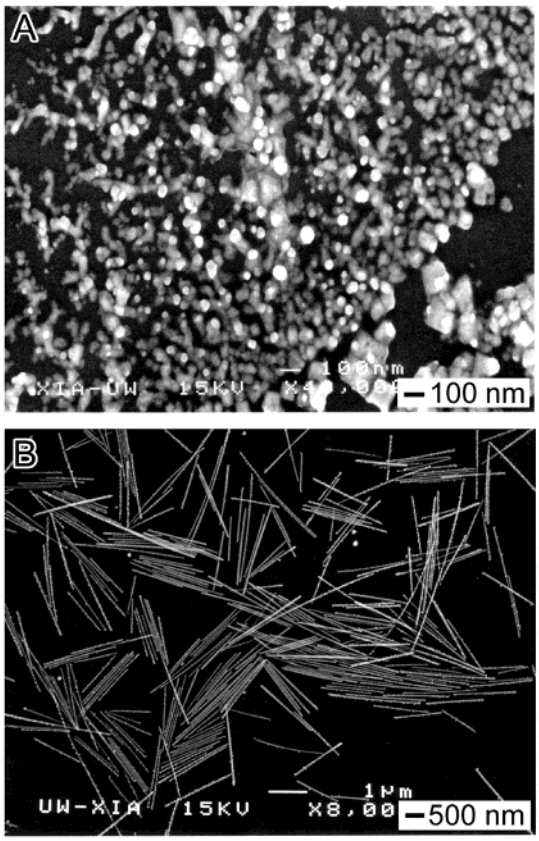

Figure 7. (A) SEM image of the product obtained after the solution was heated at 100 °C for 20 h. (B) SEM image of the product obtained when the solution was heated at 185 °C for 1 h. Other conditions were the same as those indicated in Figure 2.

Silver nanoparticles have also been used as seeds for the growth of nanostructures from several elements, e.g., copper nanoparticles and selenium nanorods.[38,39] In the present synthesis, when preformed silver nanoparticles (instead of platinum) were used as the seeds, the products were still obtained as mixtures of nanowires and nanoparticles. Figure 8B shows a typical SEM image of the sample obtained from such a process. Silver nanowires with a relatively high yield were obtained, but the distribution of diameters seemed to be broader than those obtained using Pt seeds. It is likely that the Ag seeds formed in this reaction were not as uniform as the Pt seeds. Procedures that involved no seeding step were also studied in our experiments. These reactions resemble a "self-seeding" process,[40] in which the silver nanoparticles formed at the very beginning could serve as the seeds for the following growth process. In this case, different morphologies were observed depending on the injection rates of $AgNO_3$ and PVP solutions. For example, silver nanoparticles were the only product when all the reactants were added within 0.5 min. If the injection rate was decreased, rod-shaped nanoparticles were observed. Silver nanowires with the highest aspect ratios (∼50) were obtained when the solutions were added over a period of 10 min (shown in

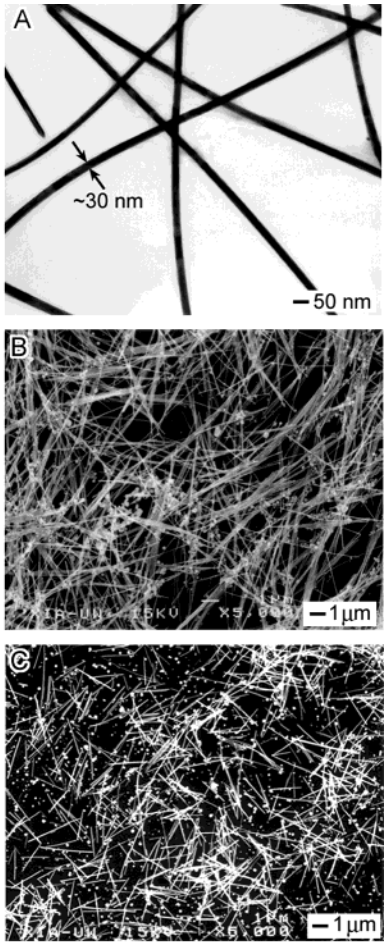

Figure 8. (A) TEM image of the product obtained when the concentration of $PtCl_2$ was increased by 10 times to 1.5×10^{-3} M. (B) SEM image of silver nanowires formed when $PtCl_2$ was replaced by $AgNO_3$ as the seeding source. (C) SEM image of the product obtained without a separated pre-seeding process. In this case, the solutions of $AgNO_3$ and PVP were injected into the reaction system over a period of 10 min. Other conditions were the same as those indicated in Figure 2.

Figure 8C). The length and number of the nanowires would decrease if the injection rate was further lowered. Figure 8C shows an SEM image of the sample obtained without pre-seeding. Here the silver nanorods had an average length of ∼2.1 μm and diameter of ∼45 nm. Compared with the nanowires obtained with Pt seeds, the diameter was slightly increased (by ∼7 nm), but the average length was significantly decreased.

Compositional and Electrical Characterization of the Silver Nanowires. To determine the actual amount of PVP covered on the silver nanowires, TGA measurements were performed on the purified samples of silver nanowires under nitrogen gas flow. The thermogravimetric (TG) curve showed a two-step weight-decline pattern (Figure 9) with the inflexion points at ∼200 and 475 °C, respectively. The first change corresponded to the desorption of solvent molecules (ethylene glycol), and the second one corresponded to the degradation of PVP that probably formed a sheath around each nanowire.[41] Typically, we observed a weight loss of ∼5.52% for EG and ∼3.44% for PVP. The EG could have been trapped in the PVP sheaths.

(38) Figlarz, M.; Ducamp-Sanguesa, C.; Fievet, F.; Lagier, J. P. *Adv. Powder Metall. Partic. Mater.* **1992**, *1*, 179.
(39) Lickes, J. P.; Dunont, F.; Buess-Herman, C. *Colloids Surf.* **1996**, *118*, 167.
(40) Sun, Y.; Xia, Y. *Adv. Mater.* **2002**, *14*, 833.
(41) Saravanan, P.; Jose, T. A.; Thomas, P. J.; Kulkarni, G. U. *Bull. Mater. Sci.* **2001**, *24*, 515.

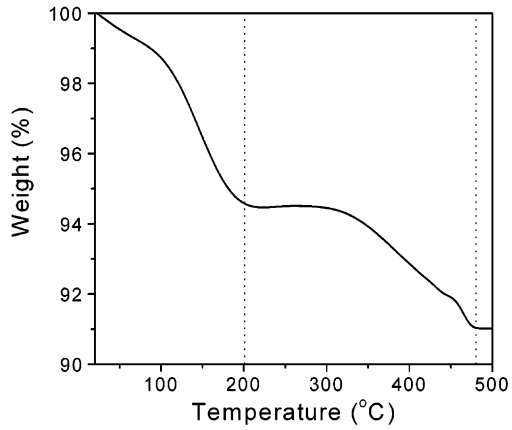

Figure 9. TG curve of the purified samples of silver nanowires. The vertical lines demarcate the regions of weight loss corresponding to ethylene glycol (at ~200 °C) and PVP (at ~475 °C).

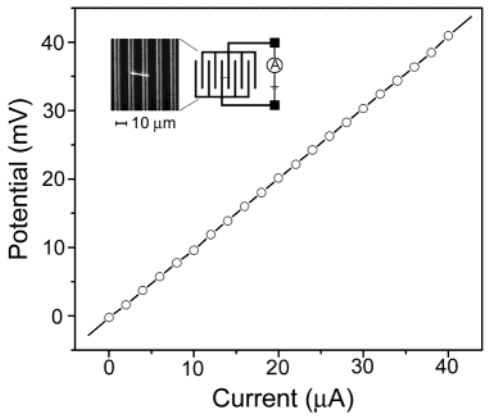

Figure 10. Electrical conductivity measurement on an individual silver nanowire that was ~40 nm in diameter. The $I-V$ curve measured on this silver nanowire could be fitted as V (mV) = 0.43 + 0.974I (μA). The insert shows an optical micrograph detailing the alignment of the silver nanowire with respect to the two parallel gold electrodes, as well as a schematic illustration of the complete experimental setup.

The quest for nanometer-scale electronics has stimulated an increasing effort in studying electron transport in metallic nanowires. We have tested the electrical continuity of these silver nanowires by measuring the resistance of an individual nanowire at room temperature using the two-probe method. In this case, a silver nanowire of ~40 nm in diameter was aligned across two gold electrodes that had been patterned on an insulating layer of silicon oxide. Current was measured while a range of DC potentials were applied to these gold electrodes. The insert of Figure 10 shows the optical microscopic image of a silver nanowire resting across two gold electrodes and a schematic drawing of the experimental design. A linear I-V curve, V (mV) = 0.43 + 0.974I (μA), was obtained (Figure 10) from which an electrical conductivity of $\sim 0.8 \times 10^5$ S/cm was calculated. This value represents a reasonable number for such a thin nanowire (the conductivity of bulk silver is 6.2×10^5 S/cm), and indicates that the bicrystalline silver nanowires synthesized using our solution-phase approach are electrically continuous, and they could serve as interconnects in fabricating nanoelectronic devices.

Conclusion

We have demonstrated a seed-assisted, solution-phase route to the large-scale synthesis of bicrystalline silver nanowires having uniform diameters in the range of 30−40 nm, and with controllable lengths up to ~50 μm. In this soft process, the evolution of silver into anisotropic nanostructures within a highly isotropic medium was mainly driven by two factors: (1) the pre-formation of metal seeds in the solution that could serve as nuclei for the subsequent growth of silver nanowires; and (2) the use of an organic polymer that could kinetically control the growth rates of various faces of *fcc* silver through chemical surface modification. Control over the lateral and longitudinal dimensions of these silver nanowires could also be achieved by varying the reaction conditions, including reaction temperature, seeding conditions, and the ratio between PVP and $AgNO_3$. Raising the reaction temperature (from 160 to 185 °C) led to the formation of short nanowires (or nanorods) with relatively low aspect ratios. An increase in the concentration of seeding solution slightly reduced the diameter of resultant nanowires. Similar to other solution-based methods, the synthetic approach described here exhibits a number of attractive features that include high yield, low cost, environmentally benign conditions with relatively low energy consumption, and relatively low temperatures (<200 °C).

Because the present reaction was carried out at ambient pressure, it can be readily scaled up for high-volume production of silver nanowires. As we have recently demonstrated, these silver nanowires could be used as templates to form new nanostructures such as uniform silica or gold nanotubes, and Ag@SiO_2 coaxial nanocables.[42] We believe that the synthetic strategy demonstrated here could also be extended to other metals because the polyol process we used here has already been applied to the synthesis of colloidal particles from a broad range of metals.[43] The major requirement seems to be the availability of appropriate polymers that are capable of forming coordination compounds with these metal ions and can selectively adsorb onto various surfaces of these metals.

Acknowledgment. This research has been supported in part by an AFOSR-DURINT subcontract from SUNY-Buffalo, a Fellowship from the David and Lucile Packard Foundation, and a Research Fellowship from the Alfred P. Sloan Foundation. Y.X. is a Camille Dreyfus Teacher Scholar (2002−2007). Y.Y. and B.M. thank the Center for Nanotechnology at the UW for the Nanotech Student Award and IGERT Fellowship (funded by the NSF, DGE-9987620), respectively. We thank Yu Lu, Hanson Fong, and Dr. Brian Reed for their help with XRD, electron diffraction, and HRTEM studies. We also thank Professor Larry Dalton for allowing us to use the TGA instrument in his research group.

CM020587B

(42) (a) Sun, Y.; Mayers, B. T.; Xia, Y. *Nano Lett.* **2002**, *2*, 481. (b) Yin, Y.; Lu, Y.; Sun, Y.; Xia, Y. *Nano Lett.* **2002**, *2*, 427.

(43) (a) Toneguzzo, P.; Viau, G.; Acher, O.; Fiévet-Vincent, F.; Fiévet, F. *Adv. Mater.* **1998**, *10*, 1032. (b) Fievet, F.; Lagier, J. P.; Blin, B.; Beaudoin, B.; Figlarz, M. *Solid State Ionics* **1989**, *32/33*, 198. (c) Ayyappan, S.; Subbanna, G. N.; Gopalan, R. S.; Rao, C. N. R. *Solid State Ionics* **1996**, *84*, 271. (d) Viau, G.; Fiévet-Vincent, F.; Fiévet, F. *Solid State Ionics* **1996**, *84*, 259. (e) Carotenuto, G.; Pepe, G. P.; Nicolais, L. *Eur. Phys. J. B* **2000**, *16*, 11.